The direct epoxidation of propene over gold–titania catalysts—A study into the kinetic mechanism and deactivation

T.A. Nijhuis *, B.M. Weckhuysen

*Utrecht University, Faculty of Science, Department for Chemistry, Section Inorganic Chemistry and Catalysis,
Sorbonnelaan 16, 3584 CA Utrecht, The Netherlands*

Abstract

A reaction scheme is presented for the epoxidation of propene over gold–titania catalysts based on information from catalytic experiments and a detailed infrared study. The reaction mechanism involves the formation of a bidentate propoxy species on titania sites by means of a reactive adsorption of propene, which is catalyzed by the gold nanoparticles. The bidentate propoxy species can react with a peroxide species, produced on the gold from hydrogen and oxygen, to produce propene oxide. Catalyst deactivation occurs via a consecutive oxidation of the bidentate propoxy intermediate to strongly adsorbed carboxylate species. A kinetic model including these reaction steps was fitted to a series of catalytic experiments and provided a good description of the measurements and yielded realistic kinetic parameters.
© 2006 Elsevier B.V. All rights reserved.

Keywords: Gold; Titania; Mechanism; Propene; Epoxidation

1. Introduction

Gold–titania catalysts are a very attractive system for the direct epoxidation of propene. Over the past years a considerable research effort has been made into this system by a large number of research groups [1–9]. Despite the fact that the performance and stability of the catalysts has improved significantly, the mechanism of the epoxidation is still largely unknown. By improving the insight in the mode of operation of this type of catalyst, the development of better catalysts for this reaction will become possible.

Propene oxide is produced over gold–titania catalysts by an oxidation in the presence of both hydrogen and oxygen. This reaction only proceeds at a relatively high rate and selectivity over catalyst which contain both gold and titania. It is assumed that one of the key steps in the reaction mechanism involves the formation of a peroxide reaction intermediate out of the hydrogen and oxygen, which would be the true oxidizing species in the reaction mechanism. This view is supported by a number papers containing theoretical work and experimental studies which have appeared recently [8,10–15]. In these papers

it is shown that gold nanoparticles are capable of producing hydrogen peroxide or adsorbed OOH intermediates. In a second part of the reaction mechanism it is assumed that this peroxide reaction intermediate epoxidizes propene over a titania site. Hydrogen peroxide is know to be able to selectively epoxidize propene over a titanium silicalite-1 (TS-1) catalyst [16]. At this moment DOW-BASF are construction a propene oxide plant in which hydrogen peroxide production and propene epoxidation over a TS-1 type catalyst are integrated in a single process [17].

This paper aims to determine key steps in the reaction mechanism of the direct propene epoxidation over gold–titania using catalytic experiments, information from and infrared study on adsorbates during adsorption and reaction experiments, and kinetic modeling.

2. Experimental

Catalysts consisting of 1 wt.% of gold on P25 titania (Degussa) were prepared by means of a deposition precipitation method [18]. The desired amount of titania was dispersed in demineralized water and the pH was adjusted to 9.5 using aqueous ammonia. Over a 30 min period a solution of $HAuCl_4$ in water was added, while maintaining a pH of 9.5 using aqueous ammonia. After aging for 30 min the catalyst was

* Corresponding author. Tel.: +31 30 2537763; fax: +31 30 2511027.
E-mail address: x.nijhuis@chem.uu.nl (T.A. Nijhuis).

washed and filtered and then dried overnight at 333 K. Finally the catalyst was calcined at 673 K for 4 h. The gold loading was verified to be the target value of 1 wt.% by performing X-ray fluorescence (XRF). Transmission electron microscopy (TEM) showed that the average particle size was 4.0 nm ($\sigma = 1.1$).

The activity of the catalyst was determined by performing experiments in a flow reactor set-up. Experiments were typically conducted with 0.3 g of catalyst at a gas flowrate of 50 ml/min (STP) of 10% of propene, 10% of oxygen and 10% of hydrogen in helium. The catalyst was tested in a number of catalytic cycles of 5 h each, with in between 1 h regenerations in 10% oxygen in helium at 573 K. The catalytic performance was tested from 313 to 573 K.

Infrared adsorption-reaction experiments were performed in a Perkin-Elmer Spectrum one transmission spectrometer on self-supporting catalyst wafers of about 100 μm thick. After drying in helium at 573 K, the cell was brought to the desired adsorption/reaction temperature (typically 323 K), after which measurements were done to determine species adsorbed on the catalyst after exposing it to epoxidation reaction conditions or an adsorbing species.

3. Catalytic experiments

In Fig. 1 the catalytic performance of the gold/titania catalyst is shown at different temperatures. At the temperatures in this figure (323–363 K) the selectivity towards propene oxide is very high, >99% at 323 K, dropping to 93% at 363 K. It can be seen that the propene conversion goes through a maximum, which is higher as the reaction temperature increases. However, the catalyst also deactivates rapidly, the rate of deactivation being higher as the temperature increases. This catalyst deactivation is completely reversible by a high temperature (573 K) treatment in oxygen/helium, after which the catalyst shows an identical behavior in a catalytic test. This indicates that the deactivation is caused by adsorbate species on the catalyst rather than by sintering of the gold nanoparticles. This was confirmed by TEM analysis of a catalyst, which had been
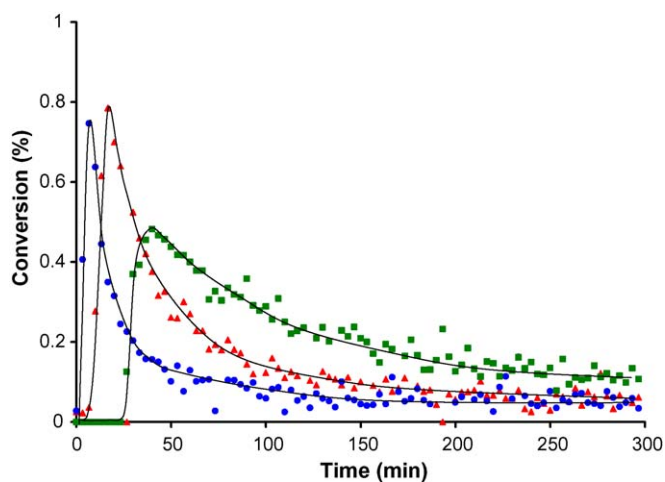
used for 300 h in epoxidation experiments. The average particles size of this catalyst (4.2 nm, $\sigma = 1.2$ nm) was within the experimental error identical to that of the fresh catalyst.

Infrared adsorption and reaction experiments showed that propene did not adsorb strongly on the titania support. Adsorption of propene oxide yielded the spectrum shown in Fig. 2A, which can be assigned to the formation of a bidentate propoxy species [19,20] on the support. This species has two very characteristic C–O–Ti vibrations at 1090 and 1140 cm^{-1} for the primary and secondary carbon atom respectively. When propene (both in presence and in absence of hydrogen/oxygen) was absorbed on the gold/titania catalyst (Fig. 2B), it could be seen that the same surface species was formed (only at 1440 cm^{-1} an additional band is present, which is discussed later). The fact that propene only adsorbed irreversible producing this bidentate propoxy species in the presence of gold nanoparticles, indicates that either propene or titania is activated by these particles. Since the presence of oxygen/hydrogen is not necessary for its formation, the oxygen in this adsorbate species must originate from the titania. The intensity of the bands for the bidentate propoxy species formed by adsorbing propene on gold/titania indicates that only on titania sites immediately surrounding the gold nanoparticles this species is formed.

The bidentate propoxy species formed when propene oxide was adsorbed on titania was found to be strongly adsorbed and stable. After up to 2 h no changes in the observed infrared spectrum were visible. The bidentate propoxy species formed upon propene adsorption on the gold/titania catalyst underwent a consecutive oxidation to carboxylate species. In Fig. 2C the
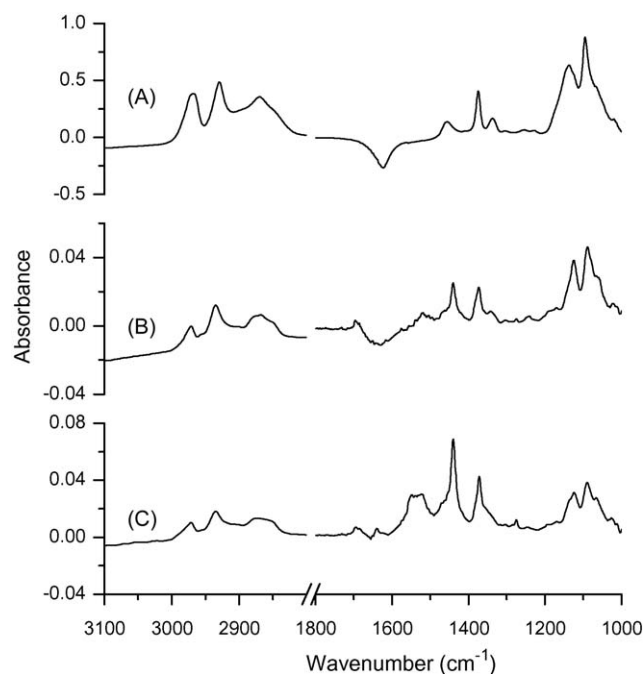

Fig. 1. Propene epoxidation over 1 wt.% Au/TiO$_2$ catalyst. Conversion of propene at 323 K (squares), 373 K (triangles) and 393 K (circles). The lines drawn through the experimental data points are meant only as a guide to the eye.

Fig. 2. Infrared adsorption–desorption experiments at 323 K. (A) Propene oxide adsorbed on TiO$_2$. (B) Propene adsorbed (reacted) on Au/TiO$_2$ (spectrum measured 5 min after 20 min propene adsorption). (C) Propene adsorbed (reacted) on Au/TiO$_2$ (spectrum measured 60 min after 20 min propene adsorption).

spectrum after propene adsorption on gold–titania is shown after 1 h. The consecutive oxidation of the bidentate propoxy to carboxylates is clear from the appearance of intense sharp bands at 1370 and 1440 cm^{-1} and a broader band at 1500–1550 cm^{-1}. At the same time a slight decrease in the CH bending and stretching vibrations could be observed. The fact that the overall intensity of the infrared vibrations of adsorbates increases can be explained by the higher sensitivity of infrared for the carboxylates compared to the adsorbed hydrocarbon species (bidentate propoxy). Since this consecutive oxidation of the bidentate propoxy species only occurred in the presence of the gold nanoparticles, it is assumed they catalyze this consecutive oxidation. The carboxylate species only desorbed very slowly from the catalyst. They could only be removed completely by heating the catalyst in the presence of oxygen to a temperature of 473 K or higher.

The bidentate propoxy species, both formed out of propene reactively adsorbing near gold particles or directly from propene oxide adsorbing, adsorbs very strongly. Only heating the sample to 573 K in the presence of oxygen caused desorption of the adsorbed propene oxide. The bidentate propoxy formed upon adsorption of propene could also be made to desorb when a hydrogen/oxygen mixture was fed to the catalyst. This latter observation is a strong indication for the fact that the bidentate propoxy species is a reaction intermediate towards propene oxide, considering the fact that at 323 K in the catalytic experiments no other products than propene oxide were formed.

Combining the information available from literature, the catalytic data, and the data from the infrared adsorption experiments, we would like to propose the reaction mechanism shown in Fig. 3. For the formation of propene oxide there are two important reaction steps. Firstly, the formation of a peroxide species on the gold nanoparticles is a key step. Secondly, there is the formation of a bidentate propoxy species as propene adsorbs on titania sites near a gold particle. The peroxide species can react with the bidentate propoxy species to produce propene oxide and re-oxidize the titania which was partially reduced when the bidentate propoxy was formed. Based on the fast formation of the bidentate propoxy species observed in the infrared experiments, the fact that a peroxide species could be observed neither in the infrared experiments nor in Raman measurements [21], and the slow desorption of the bidentate propoxy when hydrogen and oxygen are co-fed, it can be assumed that the peroxide formation is the rate determining step in this mechanism.

As a side reaction the bidentate propoxy can be oxidized further, also catalyzed by the gold nanoparticles. This reaction is the one causing the catalyst deactivation, the surface species formed by this consecutive oxidation are strongly adsorbed and only desorb very slowly or upon a catalyst regeneration by heating it in the presence of oxygen.

4. Kinetic modeling

A kinetic model based on the reaction scheme shown in Fig. 3 was derived [22]. The model is able to transiently calculate the propene oxide concentration in the gas phase and the concentrations of the relevant adsorbate species as a function of the axial position in the catalyst bed. The model was based on the assumptions that the gas phase concentrations of the reactants were constant (reasonable considering the low conversion levels). It was assumed that any peroxide species formed would immediately react with a bidentate propoxy to
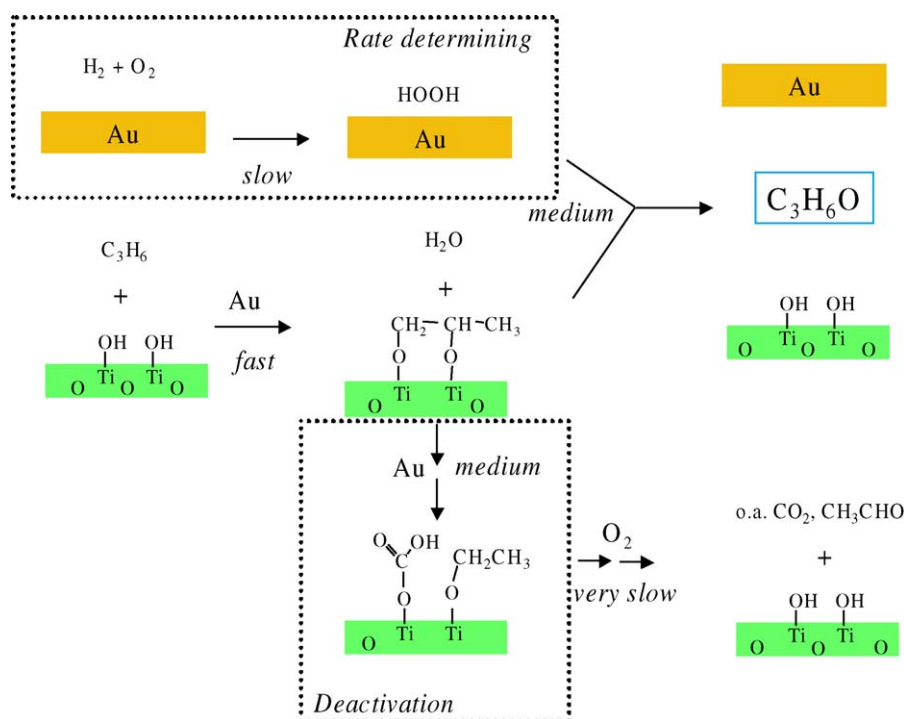

Fig. 3. Schematic representation of model for reaction and deactivation for the propene epoxidation over gold–titania catalysts.

$$\frac{\partial C_{PO}}{\partial t} = -\frac{\phi_v}{A_r \cdot \varepsilon} \cdot \frac{\partial C_{PO}}{\partial x} + \varepsilon \cdot D \cdot \frac{\partial^2 C_{PO}}{\partial x^2} - k_a \cdot C_{PO} \cdot (1 - \theta_{PO,TiAu} - \theta_{Carb,TiAu}) \cdot N_{Ti} \cdot f_{TiAu}$$
$$+ k_d \cdot N_{Ti} \cdot f_{TiAu} \cdot \theta_{PO,TiAu} - k_a \cdot C_{PO} \cdot (1 - \theta_{PO,TiTi}) \cdot N_{Ti} \cdot (1 - f_{TiAu}) \tag{1}$$

$$\frac{\partial \theta_{PO,TiAu}}{\partial t} = k_r \cdot (1 - \theta_{PO,TiAu} - \theta_{Carb,TiAu}) + k_a \cdot C_{PO} \cdot (1 - \theta_{PO,TiAu} - \theta_{Carb,TiAu}) - k_d \cdot \theta_{PO,TiAu} - k_{deact} \cdot \theta_{PO,TiAu} \tag{2}$$

$$\frac{\partial \theta_{Carb,TiAu}}{\partial t} = k_{deact} \cdot \theta_{PO,TiAu} - k_{react} \cdot \theta_{Carb,TiAu} \tag{3}$$

$$\frac{\partial \theta_{PO,TiTi}}{\partial t} = k_a \cdot C_{PO} \cdot (1 - \theta_{PO,TiTi}) \tag{4}$$

Initial and boundary conditions:

at t=0: $C_{PO}, \theta_{PO,TiAu}, \theta_{PO,TiTi}, \theta_{Carb,TiAu} = 0$

at x=0: $C_{PO} = 0$

at x=L: $\dfrac{\partial C_{PO}}{\partial x} = 0$

With			
	A_r	reactor cross sectional area	m^2
	C	gas phase concentration	mol/m^3
	D	(gas phase) diffusivity	m^2/s
	f_{TiAu}	fraction of Ti sites neighboring gold	-
	k	rate constant	$1/s$
	L	catalyst bed length	m
	N_{Ti}	Ti site concentration	mol/m^3
	t	time	s
	x	(axial) position in reactor	m
	ε	catalyst bed porosity	-
	ϕ_v	volumetric gas flow rate	m^3/s
	θ	surface occupancy	-
Subscripts:	PO	propene oxide	
	TiAu	titanium neighboring gold	
	TiTi	titanium not neighboring gold	
	a	adsorption	
	d	desorption by reaction of bidentate propoxy with peroxide species	
	r	reaction of propene forming adsorbed bidentate propoxy	
	deact	deactivation by oxidation of bidentate propoxy	
	react	catalyst reactivation by desorption of deactivating specie	

Scheme 1. Differential equations describing the kinetic model.

produce propene oxide (in line with the assumption of the peroxide formation being the rate determining step). Propene oxide can re-adsorb on both titania sites neighboring gold and on the non-catalytic sites elsewhere on the titania. The bidentate propoxy species can as a side reaction be oxidized towards carbonate/carboxylate species, causing the catalyst lose activity as the concentration of this strongly adsorbing species increases on the catalyst.

In Scheme 1 the kinetic model is presented. Eq. (1) describes the propene oxide concentration in the gas phase. The terms in the equation represent convective transport, diffusional transport, (re-)adsorption on catalytic sites, production of propene oxide from the reaction between a peroxide species and a bidentate propoxy on the catalytic sites, and adsorption on non-catalytic sites. Eq. (2) describes the concentration of the bidentate propoxy species on the catalytic sites. The terms in this equation represent the bidentate propoxy formation by reactive propene adsorption, propene oxide adsorption, propene oxide formation by reaction with a peroxide species, and the
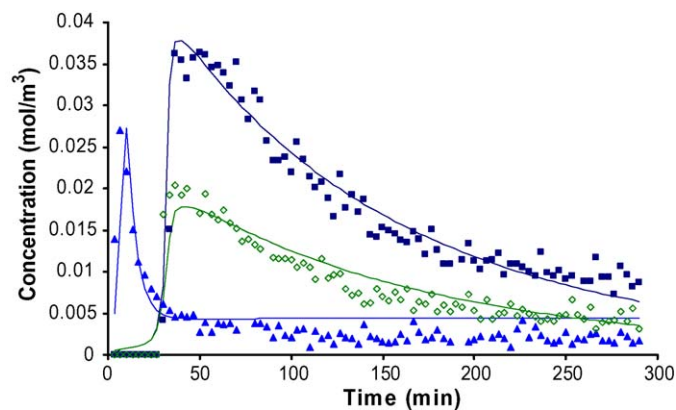

Fig. 4. Comparison of kinetic model (line) and measurements (symbols) for a number of experiments at different reaction conditions. (■) $T = 325$ K, GHSV = 3600 h^{-1}; (◇) $T = 325$ K, GHSV = 9000 h^{-1}; (▲) $T = 365$ K, GHSV = 9000 h^{-1}.

Table 1
Summary of parameters obtained from fitting the kinetic model to the experimental data set (rate constants at 325 K)

Parameter	Units	Value	95% Confidence region	
			Lower	Upper
k_r	min^{-1}	1.18	0	2.4
k_a	m^3/mol/min	70.9	25	117
k_d	min^{-1}	2.63	0	6.2
k_{deact}	min^{-1}	0.0202	0.004	0.036
k_{react}	min^{-1}	1.08×10^{-5}	8.5×10^{-6}	1.3×10^{-5}
N_{Ti}	mol/m^3	282	220	340
f_{TiAu}	–	0.043	0.005	0.081
$E_{a,r}$	kJ/mol	47.5	36	58
$E_{a,d}$	kJ/mol	46.8	24	69
$E_{a,deact}$	kJ/mol	144	133	154
$E_{a,react}$	kJ/mol	81.9	60	104

consecutive oxidation to produce carbonates/carboxylates. The third equation represents the formation of carbonates by the oxidation of bidentate propoxy species and their desorption. Eq. (4) represents the adsorption of propene oxide on non-catalytic titania sites.

The kinetic model was fitted to a large data set of experimental observations at different flowrates, catalyst masses, and temperatures (15 individual experiments with 100 experimental data points each). Once single set of reaction parameters was determined for all experiments by minimizing the squares sum of residuals between model predictions and measured observations. The model described the measurements well in the temperature range of 313–365 K, the range at which propene oxide is produced with a high selectivity. Fig. 4 shows the model and the measurements at four different experimental conditions. Only at the highest reaction temperature, where the selectivity towards propene oxide decreases, the model has a small deviation from the measurements. Side reactions were not included in to the model, which explains this deviation.

Table 1 lists the parameters as were obtained from the kinetic modeling. In literature no rate constants or activation energies are reported for the propene epoxidation over gold–titania catalysts, which could have been used as a reference. The reason for this is most likely the dynamic behavior of the catalyst during the reaction in which the catalyst activity first increases and then decreases and the seemingly negative activation energy for the reaction, since the 'steady state' activity of the catalyst decreases with an increasing temperature. This last behavior can be explained based on the activation energies in Table 1. It can be seen that the activation energy for deactivation (144 kJ/mol) is higher than the activation energies relevant for the propene oxide production (k_r and k_d, both 47 kJ/mol). This latter values are of a similar magnitude as reported values for the heat of desorption of propene from TiO$_2$ and Au/TiO$_2$ (47 and 60 kJ/mol, respectively [23]). The adsorption capacity for propene (oxide) the model calculates (282 mol/m^3, =1.4 wt.% PO) for the catalyst corresponds well to the experimentally determined adsorption capacity for this catalyst [19]. The fraction of titanium sited neighboring gold (4%) also

is a reasonable value if one looks at transmission electron microscope pictures of the catalyst.

5. Discussion

The combination of spectroscopic measurements, catalytic measurements, and kinetic modeling discussed in this paper brings the understanding of mode of operation of gold–titania catalysts for the propene epoxidation a step closer. In literature there is no agreement yet on the manner in which these catalysts work. One point on which agreement seems to have been reached, is that the main role of gold is the formation of a peroxide species or hydrogen peroxide. This has been confirmed both by experimental and theoretical studies [8,10,12–14,24]. In the model we propose, this is also an essential step, but we also propose another role for gold, namely the activation of propene, which thereafter reacts with titania surface groups [5,19,22] and only in a second step reacts with a peroxide species. The bidentate propoxy species we observed on the surface, was also observed by Mul et al. [20], but not identified as a reaction intermediate. Whether this species is indeed the important reaction intermediate as we suggest, and how this species or a different type of adsorbed propene species reacts with the peroxide species still needs further investigation.

We showed in our modeling that the strong adsorption of propene oxide on the catalyst is one of the main factors limiting the catalytic activity. This view is also confirmed in literature, where it is shown that a competitively adsorbing component can positively affect the propene epoxidation [7,25]. Furthermore, Haruta has shown that silylation of surface hydroxyls, which significantly reduces the propene oxide adsorption strength, greatly improves the propene oxide yield [26].

6. Conclusions

A mechanistic model is presented for the gold–titania catalyzed propene epoxidation, which is able to describe the catalytic measurements well. The key steps in the reaction mechanism are the formation of a bidentate propoxy species on titania upon a reactive adsorption of propene. Gold nanoparticles are essential for the formation of this species. This bidentate propoxy species consecutively can produce propene oxide by reacting with a peroxide species produced on gold from hydrogen and oxygen. Alternatively this species can be oxidized further to produce strongly adsorbed carboxylate species on the catalyst causing the catalyst to lose activity.

References

[1] Y.H. Yuan, X.G. Zhou, W. Wu, Y.R. Zhang, W.K. Yuan, L.G. Luo, Catal. Today 105 (2005) 544.

[2] B. Yoon, H. Hakkinen, U. Landman, A.S. Worz, J.M. Antonietti, S. Abbet, K. Judai, U. Heiz, Science 307 (2005) 403.

[3] E.E. Stangland, B. Taylor, R.P. Andres, W.N. Delgass, J. Phys. Chem. B 109 (2005) 2321.

[4] A.K. Sinha, S. Seelan, M. Okumura, T. Akita, S. Tsubota, M. Haruta, J. Phys. Chem. B 109 (2005) 3956.

[5] T.A. Nijhuis, T. Visser, B.M. Weckhuysen, Angew. Chem. Int. Ed. 44 (2005) 1115.

[6] G.J. Hutchings, Catal. Today 100 (2005) 55.

[7] A. Zwijnenburg, M. Makkee, J.A. Moulijn, Appl. Catal. A: Gen. 270 (2004) 49.

[8] C. Sivadinarayana, T.V. Choudhary, L.L. Daemen, J. Eckert, D.W. Goodman, J. Am. Chem. Soc. 126 (2004) 38.

[9] A.K. Sinha, S. Seelan, S. Tsubota, M. Haruta, Top. Catal. 29 (2004) 95.

[10] T. Ishihara, Y. Ohura, S. Yoshida, Y. Hata, H. Nishiguchi, Y. Takita, Appl. Catal. A: Gen. 291 (2005) 215.

[11] D.G. Barton, S.G. Podkolzin, J. Phys. Chem. B 109 (2005) 2262.

[12] D.H. Wells, W.N. Delgass, K.T. Thomson, J. Catal. 225 (2004) 69.

[13] P. Landon, P.J. Collier, A.F. Carley, D. Chadwick, A.J. Papworth, A. Burrows, C.J. Kiely, G.J. Hutchings, Phys. Chem. Chem. Phys. 5 (2003) 1917.

[14] P. Landon, P.J. Collier, A.J. Papworth, C.J. Kiely, G.J. Hutchings, Chem. Commun. (2002) 2058.

[15] P.P. Olivera, E.M. Patrito, H. Sellers, Surf. Sci. 313 (1994) 25.

[16] M.G. Clerici, G. Bellussi, U. Romano, J. Catal. 129 (1991) 159.

[17] A. Tullo, Chem. Eng. News 82 (2004) 15.

[18] T.A. Nijhuis, B.J. Huizinga, M. Makkee, J.A. Moulijn, Ind. Eng. Chem. Res. 38 (1999) 884.

[19] T.A. Nijhuis, T. Visser, B.M. Weckhuysen, J. Phys. Chem. B 109 (2005) 19309.

[20] G. Mul, A. Zwijnenburg, B. van der Linden, M. Makkee, J.A. Moulijn, J. Catal. 201 (2001) 128.

[21] R.G. Bowman, H.W. Clark, A. Kuperman, G.E. Hartwell, G.R. Meima, DOW, US, 2003.

[22] T.A. Nijhuis, T.Q. Gardner, B.M. Weckhuysen, J. Catal. 236 (2005) 153.

[23] H.M. Ajo, V.A. Bondzie, C.T. Campbell, Catal. Lett. 78 (2002) 359.

[24] A.M. Joshi, W.N. Delgass, K.T. Thomson, J. Phys. Chem. B 109 (2005) 22392.

[25] T.A. Nijhuis, B.M. Weckhuysen, Chem. Commun. 2005 (2005) 6002.

[26] A.K. Sinha, S. Seelan, S. Tsubota, M. Haruta, Angew. Chem. Int. Ed. 43 (2004) 1546.